



**HAL**  
open science

## Components interactions controlling starch–kaolinite composite films properties

Jean Aimé Mbey, Fabien Thomas

► **To cite this version:**

Jean Aimé Mbey, Fabien Thomas. Components interactions controlling starch–kaolinite composite films properties. Carbohydrate Polymers, 2014, 10.1016/j.carbpol.2014.10.053. 10.1016/j.carbpol.2014.10.053 . hal-01079322

**HAL Id: hal-01079322**

**<https://hal.science/hal-01079322>**

Submitted on 31 Oct 2014

**HAL** is a multi-disciplinary open access archive for the deposit and dissemination of scientific research documents, whether they are published or not. The documents may come from teaching and research institutions in France or abroad, or from public or private research centers.

L'archive ouverte pluridisciplinaire **HAL**, est destinée au dépôt et à la diffusion de documents scientifiques de niveau recherche, publiés ou non, émanant des établissements d'enseignement et de recherche français ou étrangers, des laboratoires publics ou privés.

## Accepted Manuscript

Title: COMPONENTS INTERACTIONS CONTROLLING  
STARCH-KAOLINITE COMPOSITE FILMS PROPERTIES

Author: J.A. Mbey F. Thomas

PII: S0144-8617(14)01065-0

DOI: <http://dx.doi.org/doi:10.1016/j.carbpol.2014.10.053>

Reference: CARP 9406



To appear in:

Received date: 3-7-2014

Revised date: 16-10-2014

Accepted date: 17-10-2014

Please cite this article as: MBEY, J. A., and THOMAS, F., COMPONENTS INTERACTIONS CONTROLLING STARCH-KAOLINITE COMPOSITE FILMS PROPERTIES, *Carbohydrate Polymers* (2014), <http://dx.doi.org/10.1016/j.carbpol.2014.10.053>

This is a PDF file of an unedited manuscript that has been accepted for publication. As a service to our customers we are providing this early version of the manuscript. The manuscript will undergo copyediting, typesetting, and review of the resulting proof before it is published in its final form. Please note that during the production process errors may be discovered which could affect the content, and all legal disclaimers that apply to the journal pertain.

1           **COMPONENTS INTERACTIONS CONTROLLING STARCH-KAOLINITE**  
2                           **COMPOSITE FILMS PROPERTIES**

3                           MBEY J. A.<sup>a,c\*</sup> and THOMAS F.<sup>a,b</sup>

4  
5       <sup>a</sup> Université de Lorraine, Laboratoire Interdisciplinaire des Environnements Continentaux,  
6       UMR 7360 , 15 Avenue du Charmois, B.P. 40. F-54501, Vandoeuvre-lès-Nancy Cedex

7       <sup>b</sup> CNRS, Laboratoire Interdisciplinaire des Environnements Continentaux, UMR 7360, 15  
8       Avenue du Charmois, B.P. 40. F-54501, Vandoeuvre-lès-Nancy Cedex

9       <sup>c</sup> The University of Yaoundé I, Department of Inorganic Chemistry, Laboratory of Applied  
10       Inorganic Chemistry, P.O. Box 812 Yaoundé

11  
12   **MBEY Jean Aimé:** [mbey25@yahoo.fr](mailto:mbey25@yahoo.fr); [jean-aime.mbey@univ-lorraine.fr](mailto:jean-aime.mbey@univ-lorraine.fr)

13   **THOMAS Fabien:** [fabien.thomas@univ-lorraine.fr](mailto:fabien.thomas@univ-lorraine.fr)

14  
15   \* Corresponding author: **e-mail:** [mbey25@yahoo.fr](mailto:mbey25@yahoo.fr) or [jean-aime.mbey@univ-lorraine.fr](mailto:jean-aime.mbey@univ-lorraine.fr)

16   Tel: +23799238925

## 17 **Abstract**

18 In order to relate the primary filler-matrix interactions to the macroscopic properties of starch-  
19 kaolinite composite material, these interactions are monitored through homo- or hetero-  
20 coagulation experiments involving both components. Turbidity measurement and Infrared  
21 spectra confirm the extreme weakness of the interactions. The addition of calcium cations  
22 shows that these weak interactions between starch and kaolinite are due to the combination of  
23 the electrostatic repulsion and hydrogen bonds formation between this two negatively charge  
24 components. Some possible relationships between the starch-kaolinite interactions and starch-  
25 kaolinite composite films properties are proposed.

26 **Keys words:** Kaolinite; Starch; Composite; Coagulation; Interface.

27

## 28 **1 : Introduction**

29 Starch and kaolinite are readily available, low cost materials that have already found uses in  
30 several domain such as composite materials (Kaewtatip and Tanrattanakul, 2012 ; Mbey et al.,  
31 2012a; Chen and Evan, 2005; de Carvalho et al., 2001; Whilem et al., 2003), paper coating  
32 (Husband, 1998), flotation of iron ore (Ma, 2011; Ma, 2010; Ma et Bruckard, 2010; Liu et al.,  
33 2000; Weissenborn et al., 1995), water treatment (Shogren, 2009 ; Bolto and Gregory, 2007 ;  
34 Krentz et al., 2006 ; Järnström et al. 1995a ; Järnström et al. 1995b). In some cases, starch  
35 undergoes some modifications prior to its use in a particular domain. Cationic starch  
36 derivatives for instance are usually of interest in flocculation of solid matter from water  
37 (Bratskaya et al., 2005 ; Chen et al., 2007 ; Wei et al., 2008 ).

38 In the domain of polymer-clay composite, the filler-polymer matrix interactions are one major  
39 key for properties change understanding. Those interactions are influenced by the filler-matrix  
40 interface and/or interphase, the filler particles orientation, the filler dosages, the filler particles  
41 anisotropy, the surface properties of the filler or the filler dispersion (Fu et al., 2008; Tran et  
42 al., 2006; Wu et al., 2002; Pukansky, 1990). In those materials, the interactions between the  
43 organic matrix and the inorganic filler determine structural and aging properties. Strong  
44 interactions guarantee rigidity and resistance to abrasion, weak interactions are required for  
45 flexibility. (Lopez et al., 2014; Müller et al., 2014; Jandas et al., 2013; Reddy et al., 2013).

46 Hence, the explanation of properties changes in composites are discussed on the basis of the  
47 filler-polymer matrix interactions. Lopez et al. (2014) associated the ductility conservation in  
48 starch-talc composite to low interactions between starch and talc particles. Müller et al.  
49 (2014), used wood particles to improve thermoplastic starch properties. They show that the  
50 wood particles having large aspect ratio improve the stiffness and the strength of the

51 composite. Also, strong interfacial adhesion between the wood particles and the starch matrix  
52 decreases the starch chains mobility and reduces the water uptake of the composite. In our  
53 previous works (Mbey et al., 2012 and 2014), unmodified or DMSO-intercalated kaolinite are  
54 used as filler in thermoplastic starch based films. The filler particle orientation and the low  
55 kaolinite dosage, together with weak kaolinite-starch interactions better account for the  
56 plasticity increase within the film. Better dispersion of the DMSO-intercalated kaolinite  
57 shows larger properties changes compared to unmodified kaolinite filled films. It is then  
58 believed that analysing the primary interactions between the components of the composite  
59 may be useful to understand the composite properties. Hence, in the case of kaolinite-  
60 thermoplastic starch composite, the study of starch-kaolinite interactions is of interest.

61 To date, general studies on the kaolinite-starch interactions are rare (Ma, 2011; Ma, 2010; Ma  
62 et Bruckard, 2010), especially in the field of starch-clay composites. In fact, those interactions  
63 are described as very weak, since the essentially non ionic hydroxylic functions available on  
64 both starch and clay interface give rise to physical sorption through hydrogen bonds.

65 For this study, we will attempt to correlate the starch-kaolinite interactions to the properties of  
66 starch-kaolinite composite films.

67 This study aims at monitoring the adsorption of cassava starch onto kaolinite as a way to  
68 understand the starch-kaolinite films properties. The dispersion or the coagulation of the  
69 kaolinite phase during composite processing will largely depend on the kaolinite-starch  
70 interactions. Absence of interactions could favour phase separation between the two  
71 components, whereas strong interactions may induce the coagulation of the clay within the  
72 polymer matrix or increase the polymers chain rigidity within the composite. On this basis, it  
73 is then obvious that weak to medium interactions are preferred for viscoelastic composite  
74 films making. To access the starch-kaolinite interactions, the sedimentation/flocculation test  
75 of dilute kaolinite suspension in presence of natural cassava starch is used.

76

## 77 **2 : Experimental section**

### 78 ***2-1: The Kaolinite material***

79 The raw kaolinite was collected from a deposit situated in Mayouom (western Cameroon)  
80 (Njoya et al., 2006). The sample used in the present study was taken at 3 m depth. The  
81 fraction < 40  $\mu\text{m}$ , labelled K3, was collected by means of wet sieving. Using inductive  
82 coupled plasma by atomic emission spectrometry (ICP-AES) to analyze the major elemental  
83 composition of the sample, an approximation of the structural formula of the kaolinite phase

84 was found to be  $(Al_{1.94} Fe_{0.06})(Si_{1.98} Fe_{0.02})O_5(OH)_4(Mg_{0.02} Ca_{0.002})$ . The mineralogical  
85 composition of the sample is as follows: Kaolinite 83.3 %; Illite 10.4 %; Titanium oxide 3.4  
86 %. The fine clay fraction was collected through sedimentation after Stokes' law. The particle  
87 size distribution of the collected fraction was analysed using a Sympatec laser diffraction  
88 granulometer equipped with the HELOS optical system and the WINDOX software for data  
89 acquisition. The average particle size (D50) was found to be 4.5  $\mu m$  and more than 80 % of  
90 the material has size less than 7.5  $\mu m$ . The BET specific surface area, determined by nitrogen  
91 adsorption using an automatic homemade apparatus, was  $(25.9 \pm 0.1) m^2/g$ . The cation  
92 exchange capacity (CEC) was measured using hexaminecobalt(III) chloride  $[Co(NH_3)_6Cl_3]$ .  
93 The amount of hexaminecobalt(III) sorbed by the solid phase was determined by colorimetric  
94 measurement at 472 nm using UV-vis spectroscopy and the CEC was found to be 6.0  
95 meq/100g.

96

### 97 **2-2: The starch material**

98 The cassava starch was obtained by aqueous extraction from cassava tubers produced in  
99 Mambando (Centre Cameroon). Starch material was manually ground and sieved at 100  $\mu m$ .  
100 The sieved starch was stored in high density polyethylene container at ambient temperature.  
101 The moisture content, determined by drying to constant weight at 105°C, is 14 %. Content in  
102 mineral ashes, determined by ignition at 550 °C in a muffle furnace, is 0.3 %. Elemental  
103 analysis using the CHNS analyser Carlo Erba 1108, indicated respective contents of carbon  
104 (39.1 %), hydrogen (7.5 %) and nitrogen (0.05 %). The H/C ratio, 5.2 is common for  
105 polysaccharides. The very low nitrogen content, and the absence of the characteristic amine  
106 band in the FTIR spectrum (not presented) indicate negligible content of proteins.

### 107 **2-3: Experimental procedures**

108 The kaolinite suspension was prepared by dilution of the aqueous extract of fine clay fraction  
109 to a solid concentration of 0.5 mg/mL of turbidity 235 NTU (HACH 2100 N turbidimeter).  
110 The starch solution was prepared by dissolving 100 mg of starch in 5 mL of analytical grade  
111 DMSO (Sigma Aldrich 99.99 %) under heating at 60 °C during 5 min. The mixture was then  
112 diluted with deionised water ( $18.2 M\Omega cm^{-1}$ ) to obtain 100 mL of solution (starch  
113 concentration 1 mg/mL). The dissolution with DMSO prevents alteration of the chemical  
114 functions and degradation of the carbohydrate chains (Han et Lim, 2004). The working pH  
115 was selected after analysing its effect on the sedimentation of the kaolinite suspension.  
116 Typically 30 mL of the initial suspension having 235 NTU turbidity was taken and used at the

117 spontaneous pH reached by the suspension (6.02) or after adjusting the pH value by adding  
118 aliquot of 0.1 M solution of either NaOH or HNO<sub>3</sub>. The samples are left for sedimentation  
119 during 40 min after which 15 mL of the suspension supernatant was taken using a  
120 micropipette for turbidity measurements. On figure 1, are reported the results obtained. It can  
121 be noted that the turbidity is stabilized around 160 NTU. This reduction of turbidity is caused  
122 by the settling of large particles that arise from collision between the clay particles subject to  
123 Brownian motion. The acid or alkaline value of pH induced either protonation or  
124 deprotonation of edge functions (=AlO-H and =SiO-H). Given that the permanent charge of  
125 the clay is negative, hence deprotonation of the edge functions, in alkaline pH, increasing the  
126 global negative charge of the suspension which result in an increase electrostatic repulsion  
127 that prevent particles collision and hence, stabilized the suspension. Conversely, in acid pH,  
128 the edge functions are positively charge inducing then a reduction of the global electrostatic  
129 repulsion. This charge reduction favours collision that result in increase particle size that  
130 settled under their weight. This explains why, acid pH favours the sedimentation and alkaline  
131 pH slightly increases suspension stability. Intermediate pH, reached spontaneously by the  
132 kaolinite suspension (pH = 6.2), was considered as an optimal starting condition for further  
133 coagulation experiments.

134 The proton surface excess of both kaolinite and starch was measured by acid-base titration  
135 using a Metrohm Titrando 809 station with two dosing units Dosino 800. The system is  
136 automatically driven by the software Tiamo (version 1.2.1 light). The titration of the  
137 suspension was carried out under magnetic stirring and argon stream to avoid carbon dioxide  
138 dissolution in the suspension. Electrophoretic mobility of the kaolinite and the starch  
139 materials was measured in NaNO<sub>3</sub> background electrolyte (10<sup>-3</sup> M, 10<sup>-2</sup> M and 10<sup>-1</sup> M) and in  
140 the presence of varying amounts of CaCl<sub>2</sub> using a Zetaphoremeter V by CAD Instrumentation  
141 (France).

142 For the sedimentation tests, 30 mL of the kaolinite suspensions was magnetically stirred for 5  
143 min after addition of known dosages of starch and CaCl<sub>2</sub>. The samples were then placed in  
144 vertical test tubes for sedimentation. After 40 min, 15 mL of the supernatant suspensions was  
145 taken for turbidity measurement using HACH 2100 N turbidimeter. The remaining  
146 suspensions were freeze-dried and the sediment conditioned in KBr pellets were analysed by  
147 FTIR. The FTIR spectra were recorded using a Bruker IFS 55 interferometer in transmission  
148 mode. The sedimentation tests were done in absence or in presence of calcium. A preliminary  
149 test of coagulation by calcium ions was done to determine the dosage to be used.

150 Uv-vis spectrometer, SHIMADZU UV 2101 PC, was used for kinetic monitoring of the

151 suspensions sedimentation. The measurements were done at 300 nm.

### 152 **3 : Result and discussion**

#### 153 **3.1: Starch-Kaolinite interactions**

154 The titration curves presented in figure 2, show the pH-dependence of the net proton surface  
155 excess. For the starch, the specific amount of acidic groups is around 43  $\mu\text{mol/g}$  (figure 2b).  
156 In order to evaluate the spatial distribution of charges on the starch macromolecule, we can  
157 assume that the latter is composed of glucose residues of molar mass 180 g/mol. The obtained  
158 charge is then 7.7 mmol of protons per mole of glucose residue, which represents 0.77 % of  
159 carboxylated residues (less than 1 % of glucose residues are bind to carboxylate group).

160 The titration curves at different ionic strength are virtually superimposed, which indicates a  
161 very low charge.

162 The titration curve of kaolinite quantifies the pH-dependent charges on the edges of the  
163 particles ( $=\text{A}-\text{O}-$  and  $=\text{SiO}-$ ), resulting in a proton surface excess of about 50  $\mu\text{mol/g}$  (figure  
164 2a). This surface charge is in accordance with the commonly observed cationic exchange  
165 capacity for kaolinites, generally below 10 meq/100g (Eslinger and Pevear, 1988, after Martin  
166 and Dacy, 2004). The fact that no common intersection point is observed on the titration  
167 curves at different ionic strength indicates the presence of small amount of permanent charge  
168 due to isomorphic substitutions in the crystalline structure of the kaolinite. Similar behaviour  
169 was observed and modelled for montmorillinites and illites by Delhorme et al. (2010) and  
170 could be attributed to the 10% of illite contained in the sample.

171 From electrophoretic mobility measurements (figure 3), it is shown that the surface charge of  
172 both starch and kaolinite is negative in the pH range of 3 to 10. The electrophoretic mobility  
173 of the starch (figure 3b) shows positive values for pH below 2.1, which indicates the presence  
174 of cationic functions such as ammonium functions in proteins, which were detected in very  
175 low amount by elemental analysis (§2.2). The negative values and pH dependence of the  
176 electrophoretic mobility of starch in the pH domain 2.5 – 7 is probably due to the dissociation  
177 of carboxylic groups on the starch macromolecules.

178 The electrophoretic mobility of kaolinite (Figure 3a) shows very little dependence on ionic  
179 strength and also on pH in the domain above pH 6, which confirms the presence of permanent  
180 charges that were detected from the titration curves. In the domain below pH 6, strong pH  
181 dependence of the electrophoretic mobility results from the protonation of the hydroxylic  
182 functions on the edges of the clay particles.



183 Adsorption isotherms are generally used to study the mechanism and strength of interaction  
184 between a mineral interface and an organic (macro)molecule. In the present case, such  
185 approach is ineffective for at least two reasons. Firstly, the weakness of the interactions does  
186 not allow strong amounts of organics to be adsorbed on the solid, as shown in published  
187 studies (Liu, 2007; Mpofu et al., 2003; Järnström et al. 1995a). Secondly, in the present study,  
188 cassava starch was used in the native form, therefore heterocoagulation experiments are more  
189 adapted than adsorption isotherms to study organo-mineral interactions. In figure 4, the  
190 turbidity of a kaolinite suspension is independent of the amount of added starch up to 2.5%  
191 (higher amounts would increase the turbidity due to the granular character of starch). Addition  
192 of  $10^{-5}$  M  $\text{CaCl}_2$  results in significant and rapid (40 minutes) sedimentation of the suspension,  
193 which confirms that electrostatic repulsions must be overcome to achieve attractive  
194 interactions, as also reported by Ma (2010). It is obvious that for dosage between 1 % and 1.5  
195 %, the effect of starch on the sedimentation is maximal. In this study, the calcium ion acts as  
196 neutralizer of the kaolinite surface charge, and the screening of the kaolinite charge favours  
197 the starch adsorption on the kaolinite surface.

198 The increase in adsorption of starch is evidenced by the decrease in the turbidity (increase  
199 sedimentation of the clay) for the same starch concentration in presence of calcium ion (figure  
200 4). The starch adsorption is almost maximal early at 0.33 % dosage of starch. It seems that  
201 adsorption of starch at low dosage is possible and this helps the kaolinite sedimentation.  
202 However, the adhesion forces are not strong enough and this explains the turbidity fluctuation  
203 observed around 1 %. Weak interactions take place in the system due to combine effect of  
204 hydrogen bonds between the two components and electrostatic repulsion between starch and  
205 kaolinite due to their negative surface charge. The hydrogen bonds could be beneficially  
206 increase by the reduction of the interaction sphere (that is, a reduction of the volume in which  
207 starch and kaolinite interact). Hence, the screening of the kaolinite surface charge by the  
208 calcium cations induce then an increase in starch adsorption. The effect of calcium ions on the  
209 electrostatic interactions between the clay and the starch is illustrated in figure 3 (c and d).  
210 While kaolinite showed to be relatively insensitive to monovalent cations ( $\text{Na}^+$ ) (Figure 3a),  
211 its negative electrophoretic mobility dramatically decreases in the presence of  $10^{-5}$  M  $\text{Ca}^{2+}$ .  
212 Comparatively, the mobility of starch is less sensitive to the presence of  $\text{Ca}^{2+}$ , the  
213 complexation of which with carboxyl and eventually dissociated hydroxyls being much  
214 weaker than on dissociated surface sites on clay. The charge interaction between kaolinite  
215 and starch is hence, reduced and this results in a decrease of the interaction sphere between  
216 kaolinite and starch that favours starch adsorption. However, one can easily note that the clay

217 surface charge remains negative even in the presence of calcium (figure 3c) as well as the  
218 starch surface (figure 3d). The hypothesis to explain the remaining negative charge of the  
219 kaolinite in the presence of calcium is that, edge-edge aggregation that leads to loose  
220 aggregates takes place within the kaolinite suspension in presence of calcium. These loose  
221 aggregates enclose part of the negative charge of kaolinite particles preventing then further  
222 screening because of the repulsion between the calcium cation at the external shell of these  
223 aggregates. Hence, even if the added calcium cations screened both starch and kaolinite  
224 surface, the overall surface of both component remain negative and the electrostatic repulsion  
225 between the two components is dominant and favours the stability of the system.

226 FTIR spectra of the raw kaolinite and aggregated sediments are presented in figure 5. The  
227 presence of the band at  $1383\text{ cm}^{-1}$  characterising the C-H bending in the pyranose ring  
228 (Velraj et al., 2011) is a proof of some starch adsorption onto kaolinite particles. However, as  
229 concluded from turbidity measurements, the amount of starch adsorbed is low. The sediments  
230 are mostly made of kaolinite as shown by the similarity between the raw kaolinite spectra and  
231 that of the freeze-dried sediments. The absence of the band at  $1383\text{ cm}^{-1}$  on the sediment  
232 obtained with 2 % starch, is probably due to the loose nature of the aggregate which agree  
233 with the previously mentioned weak adhesion force between the two components. It is  
234 proposed that natural gravimetric sedimentation is dominant and the contribution of potential  
235 coagulation due to both starch and calcium is low.

236 The kinetic evidence of the influence of starch on the kaolinite sedimentation is presented on  
237 figure 6. The difference between the blank system and systems containing starch, calcium or  
238 starch + calcium is obvious. The starting of sedimentation is effective between 10 min and 15  
239 min. The kaolinite sedimentation is increase in the presence of starch. The addition of calcium  
240 ameliorate the starch adsorption on the clay which better promotes the kaolinite  
241 sedimentation. The increase sedimentation due to starch adsorption is rather low indicating  
242 weak adhesion interactions that are clearly related to the surface state of both components  
243 which are negatively charged.

### 244 ***3.2: Relating the starch-kaolinite interactions to the starch-kaolinite films properties***

245 In the aim of understanding the properties of composite films, a global view of weak starch-  
246 kaolinite interfacial interactions can explain the good dispersion of the kaolinite within the  
247 starch matrix. This view of weak interactions is regarded as a result of the predominance of  
248 the electrostatic repulsion between these two negatively charged components and the H-bonds  
249 formation due to the existence of hydroxyl groups on the surface of both components. In  
250 particular, the existence of electrostatic repulsion is favourable to the clay dispersion. The

251 presence of kaolinite between the starch chains with weak kaolinite-starch interactions  
252 facilitates the mobility of the starch chains, giving rise to a plasticizing effect of the clay  
253 within the starch matrix. These hypotheses correlate well with the decrease of the glass  
254 transition temperature reported in a previous work (Mbey et al., 2012). The glycerol  
255 molecules, present at the starch-kaolinite interface, may also participate in the interactions  
256 within the films network.

257 Due to the electrostatic repulsion between the two components, the clay particles are better  
258 oriented in the starch matrix in the direction that minimizes the repulsion between the two  
259 components. Because kaolinite charge is supposed to be more dense on edges surfaces, a  
260 preferential basal orientation of the kaolinite particles is expected within the films (figure 7a).  
261 Such an orientation may also contribute to an increase in starch chain mobility through an  
262 increase of the plasticizer diffusion and prevention of plasticizer escape. The optical  
263 micrograph presented in figure 7b, actually corroborates such an orientation. This orientation  
264 also agrees well with barrier properties to water uptake, heat diffusion or UV-light  
265 transmission (Mbey et al., 2012). More recently (Mbey et al., 2014), tensile test  
266 measurements indicate a decrease in ultimate tensile strength and elastic modulus, in  
267 accordance with the decrease of the glass transition temperature previously reported (Mbey et  
268 al., 2012). These changes also corroborate the weak starch-kaolinite interactions that allows  
269 better gliding of the starch chains and a basal orientation of the clay particles which are  
270 consistent with the increase plasticizing effect due to the kaolinite. On figure 8, the  
271 experimental evaluation of some critical films properties, namely glass transition temperature  
272 and ultimate tensile strength evolution with clay content in the composite films, are given  
273 (Mbey et al., 2012 and 2014) to reinforce the propose qualitative correlation of the interfacial  
274 interactions with the macroscopic properties.

#### 275 4 : **Conclusion**

276 This study shows possible links between filler-polymer matrix interactions and starch-  
277 kaolinite composite films properties. Weak starch-kaolinite interactions, that result from  
278 electrostatic repulsion combined to hydrogen bonds formation, evidenced from coagulation  
279 tests corroborate the weak interfacial interactions in the composites films. These weak  
280 interactions are favourable to preferential basal orientation of clay particles within the film  
281 and improve dispersion of the filler. All of which agree with the reported improve  
282 plasticization and water uptake, UV light and heat diffusion barrier (Mbey et al., 2012 and  
283 2014). Hence, the dependency of the material properties of the starch-kaolinite film to  
284 components interactions is better evidenced. As reported in the literature, this work also

285 contributes to evidence the fact that composite material properties are dependent on the  
286 interactions between the constituents of the composites.

287

Accepted Manuscript

287 Acknowledgements:

288 Celine Caillet is greatly thanked for her help in titrations experiments.

289

Accepted Manuscript

289 **References**

- 290 Bratskaya S., Schwarz S., Liebert T. et Heinzec T. (2005). Starch derivatives of high degree  
291 of functionalization 10. Flocculation of kaolin dispersions. *Colloids and Surfaces, A* 254, 75–  
292 80.
- 293 Bolto B. and Gregory J. (2007). Organic polyelectrolytes in water treatment. *Water research*,  
294 41, 2301-2324.
- 295 Chen B. and Evans J. R. G. (2005), Thermoplastic starch–clay nanocomposites and their  
296 characteristics, *Carbohydrate Polymers*, 61, 455- 463.
- 297 Chen Y., Liu S. and Wang G. (2007). A kinetic investigation of cationic starch adsorption  
298 and flocculation in kaolin suspension. *Chemical Engineering Journal*, 133, 325–333.
- 299 De Carvalho, A. J. F., Curvelo, A. A. S. and Agnelli, J. A. M., (2001). A first insight on  
300 composites of thermoplastic starch and Kaolin. *Carbohydrate Polymers*. 45, 189-194.
- 301 Delhorme M., Labbez C., Caillet C., Thomas F. (2010) : Modelling acid-base properties of  
302 2:1 clays. The role of electrostatics. *Langmuir* 26 (240-9249)
- 303 Fu S-Y, Feng X-Q, Lauke B. and Mai Y-W., (2008) Effects of particle size, particle/matrix  
304 interface adhesion and particle loading on mechanical properties of particulate–polymer  
305 composites. *Composites: part B*, 39, 933–961
- 306 Jandas P.J., Mohanty S. and Nayak S.K., (2013). Surface treated banana fiber reinforced poly  
307 (lactic acid) nanocomposites for disposable applications. *Journal of cleaner production*, 52,  
308 392-401.
- 309 Järnström L., Lason L., Rigdahl M. (1995)a. Flocculation in kaolin suspensions induced by  
310 modified starches 1. Cationically modified starch-effects of temperature and ionic strength.  
311 *Colloids and Surfaces A : Physicochemical and Engineering Aspects*. 104, 191-205.
- 312 Järnström L., Lason L., Rigdahl M.. (1995) b. Flocculation in kaolin suspensions induced by  
313 modified starches 2. Oxidized and hydrophobically modified oxidized starch in comparison  
314 with poly(vinyl alcohol) and carboxymethylcellulose. *Colloids and Surfaces, A*104, 207-216.
- 315 Han J-A and Lim S-T, (2004). Structural changes of corn starches by heating and stirring in  
316 DMSO measured by SEC-MALLS-RI system. *Carbohydrate Polymers*, 55, 265–272.
- 317 Kaewtatip K. and Tanrattanakul V., (2012). Structure and properties of pregelatinized cassava  
318 starch/kaolin composites, *Materials and Design*, 37, 423–428.
- 319 Krentz D.O., Lohmann C, Schwarz S., Bratskaya S., Liebert T., Laube J., Heinze T, Kulicke  
320 W-M. (2006). Properties and Flocculation Efficiency of Highly Cationized Starch  
321 Derivatives. *Starch/Stärke*. 58, 161–169.
- 322 Liu P., (2007). Polymer modified clay minerals: A review. *Applied Clay Science*, 38, 64–76.

- 323 López, O.V., Castillo, L.A., García, M.A., Villar, M.A., Barbosa, S.E., (2014). Food  
324 packaging bags based on thermoplastic corn starch reinforced with talc nanoparticles, *Food*  
325 *Hydrocolloids*, doi: 10.1016/j.foodhyd.2014.04.021.
- 326 Ma M. (2011, May 30). Starch-kaolinite Interactions. *SciTopics*. Retrieved January 27, 2012,  
327 from [http://www.scitopics.com/Starch\\_kaolinite\\_Interactions.html](http://www.scitopics.com/Starch_kaolinite_Interactions.html)
- 328 Ma X. (2010). Role of hydrolyzable metal cations in starch–kaolinite interactions.  
329 *International Journal of Mineral Processing*, 97, 100–103.
- 330 Ma X. and Bruckard W. J. (2010). The effect of pH and ionic strength on starch–kaolinite  
331 interactions. *International Journal of Mineral Processing*, 94, 111–114.
- 332 Martin P. and Dacy J., 2004. Effective  $Q_v$  by NMR core tests. SPWLA 45th Annual Logging  
333 Symposium, June 6-9, 2004.
- 334 Mbey J. A., Hoppe S. and Thomas F. (2012). Cassava-starch kaolinite composite film. Effect  
335 of clay content and clay modification on film properties. *Carbohydrate polymers*, 88, 213-  
336 222.
- 337 Mbey J. A., Hoppe S. and Thomas F. (2014). Cassava-starch kaolinite composite film.  
338 Thermal and mechanical properties related to filler-matrix interactions. In Press, *Polymer*  
339 *Composites*, DOI 10.1002/pc.22928.
- 340 Mporu P., Addai-Mensah J., Ralston J. (2003). Investigation of the effect of polymer  
341 structure type on flocculation, rheology and dewatering behaviour of kaolinite dispersions.  
342 *International Journal of Mineral Processing*, 71, 247– 268.
- 343 Müller P., Renner K., Moczo J., Fekete E. and Pukanszky B., (2014). Thermoplastic  
344 starch/wood composites: Interfacial interactions and functional properties. *Carbohydrate*  
345 *Polymers*, 102, 821– 829.
- 346 Njoya A., Nkoumbou C., Grosbois C., Njopwouo D., Njoya D., Courtin-Nomade A., Yvon J.,  
347 and Martin F. (2006). Genesis of Mayouom kaolin deposit (western Cameroon). *Applied Clay*  
348 *Science*, 32, 125-140.
- 349 Pukanszky B., (1990). Influence of interface interaction on the ultimate tensile properties of  
350 polymer composites. *Composites*, 21(3), 255-262.
- 351 Reddy M.M., Vivekanandhana S., Misra M., Bhatia S.K. and Mohanty A.K., (2013).  
352 Biobased plastics and bionanocomposites: Current status and future opportunities. *Progress in*  
353 *polymer Science*, 38, 1653– 1689.
- 354 Shogren R.L. (2009). Flocculation of kaolin by waxy maize starch phosphates. *Carbohydrate*  
355 *Polymers*. 76, 639–644.

- 356 Tran N.H., Wilson M.A., Milev A.S., Dennis G.R., Kannangara G.S.K. and Lam R.N.,  
357 (2006). Dispersion of silicate nano-plates within poly(acrylic acid) and their interfacial  
358 interactions. *Science and Technology of Advanced Materials*, 7, 786–791.
- 359 Velraj G., Ramya R. and Nazni P., (2011). Fourier Transform Infrared Spectroscopic Study  
360 on Glycoalkaloid Concentration in Varieties of *Solanum tuberosum*. *Journal of Experimental*  
361 *Sciences*, 2(2), 68-71.
- 362 Weissenborn, P.K., Warren, L.J., Dunn, J.G., 1995. Selective flocculation of ultrafine iron  
363 ore. Part 1. Mechanism of adsorption of starch onto hematite. *Colloids and Surface*, A99,  
364 11–27.
- 365 Wei Y., Cheng F. and Zheng H. (2008). Synthesis and flocculating properties of cationic  
366 starch derivatives. *Carbohydrate polymers*, 74, 673–679.
- 367 Wilhelm, H. M., Sierakowski, M. R., Souza, G. P., and Wypych, F. (2003). The influenced of  
368 layered compounds on the properties of starch/layered compounds composites. *Polymer*  
369 *International*, 52, 1035-1044.
- 370 Wu C.L., Zhang M.Q., Rong M.Z. and Firedrich K., (2002). Tensile performance  
371 improvement of low nanoparticles filled-polypropylene composites. *Composites science and*  
372 *technology*, 62, 1327–1340.
- 373



373

374

375 cassava starch and kaolinite properties > origins and intensities of interactions> Interfacial  
376 interactions related to starch-kaolinite composite films properties

377

Accepted Manuscript

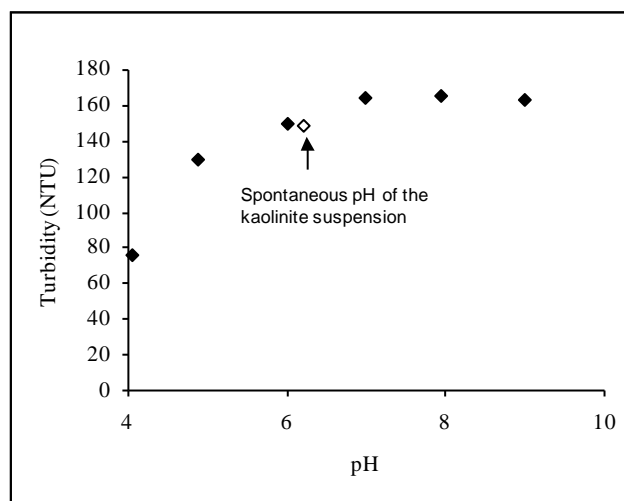


Figure 1: Analysis of the pH effect on the sedimentation of the kaolinite suspension

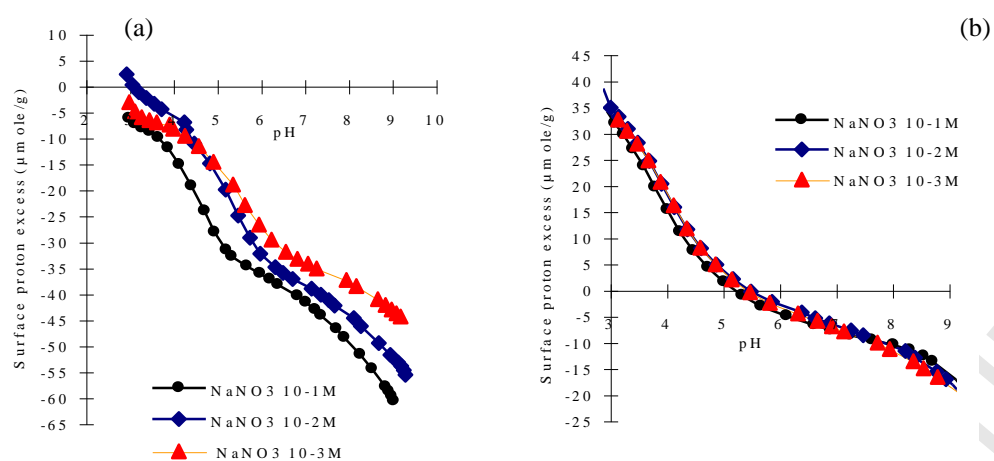


Figure 2: Surface proton excess for the kaolinite ( $\sim 50 \mu\text{mol/g}$ ) (a) and the cassava starch ( $\sim 43 \mu\text{mol/g}$ ) (b) as a function of pH and ionic strength

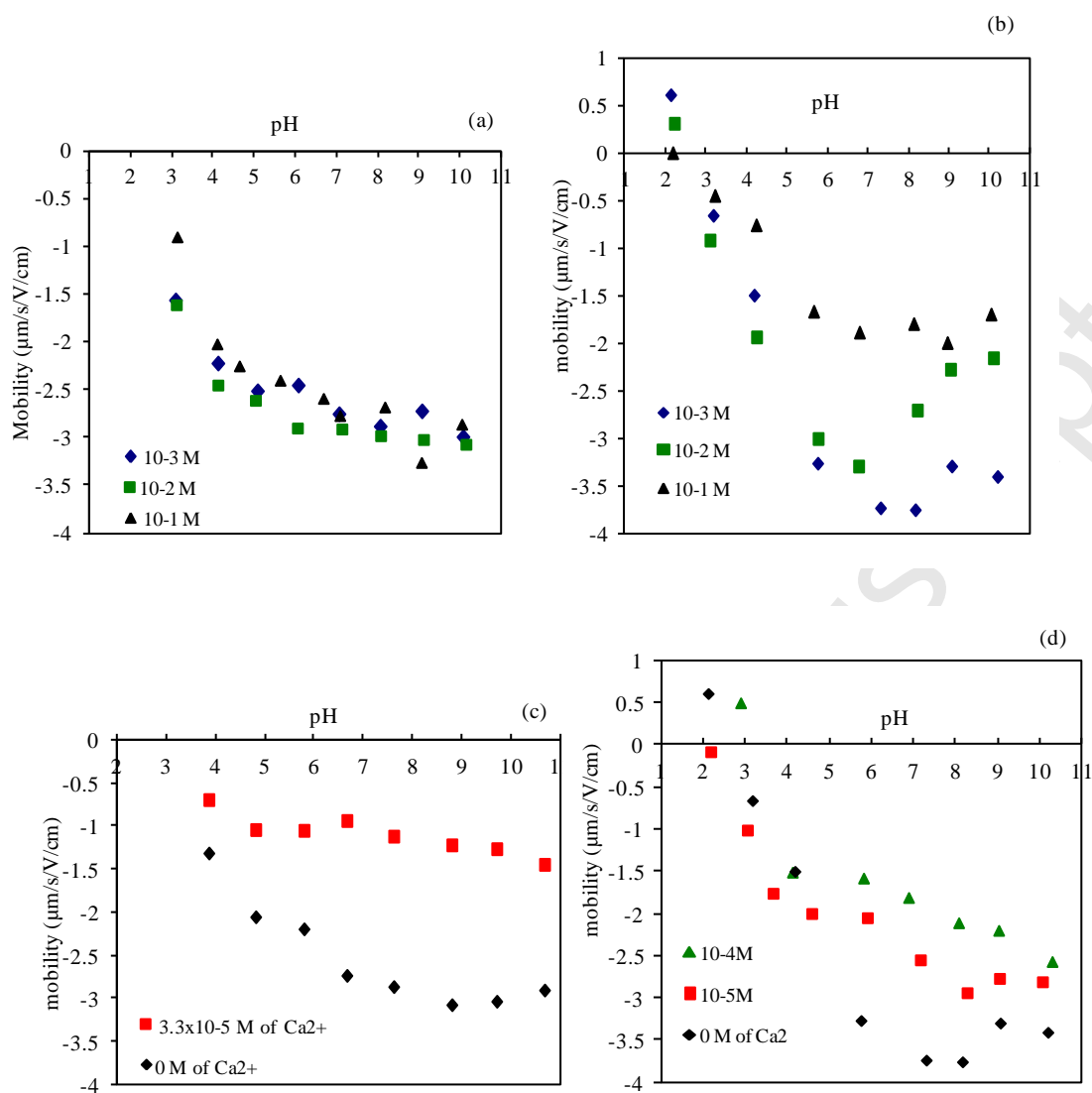


Figure 3: Electrophoretic mobility of the kaolinite (a) and the starch (b) in  $\text{NaNO}_3$  background and mobility of kaolinite (c) and starch (d) in presence of calcium cations

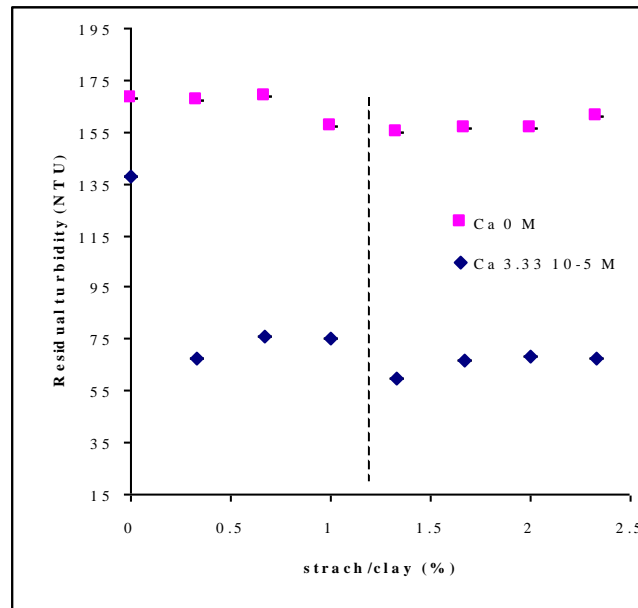


Figure 4: Turbidity measurements after 40 min sedimentation of kaolinite suspension (starting turbidity of the kaolinite suspension 235 NTU)

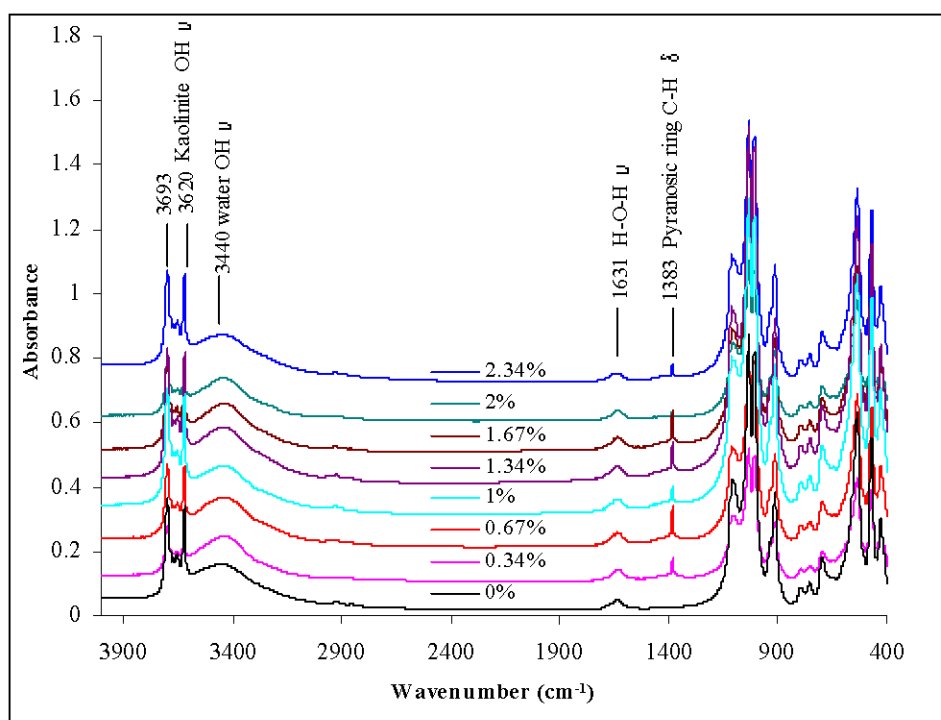


Figure 5: Infrared spectra of the kaolin-starch sediments ( $\nu$ : stretching;  $\delta$ : bending)

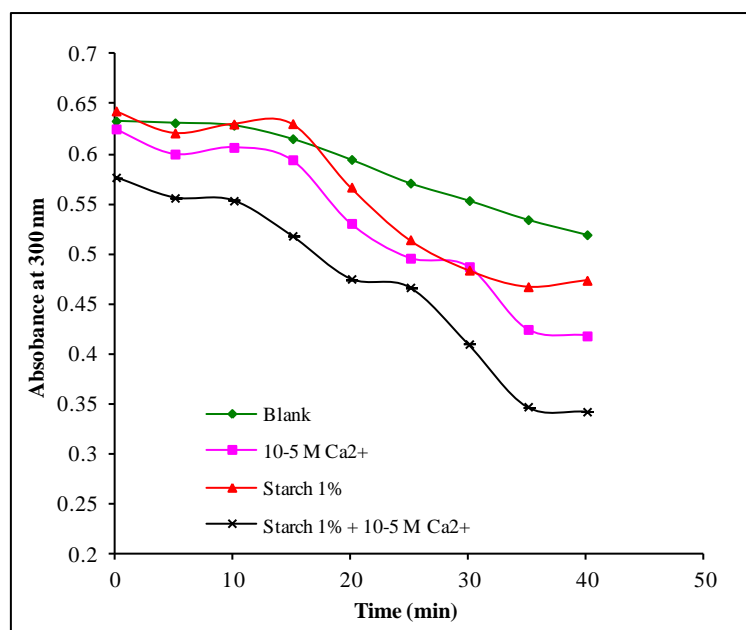


Figure 6: Uv-vis kinetic profile during kaolinite sedimentation

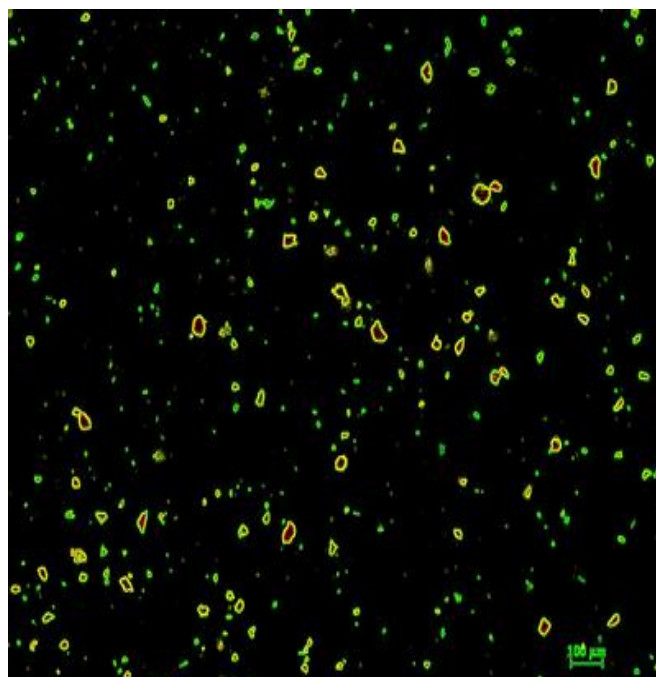
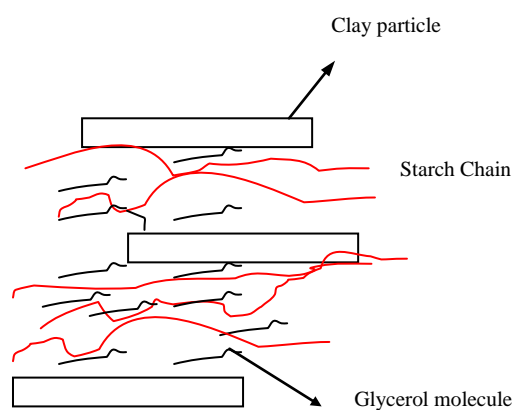


Figure 7: (a) Illustration of clay-starch interface in the composite film (b) optical micrograph of 10 % loaded kaolinite cassava starch composite film analyzed for form enhancement using image J.



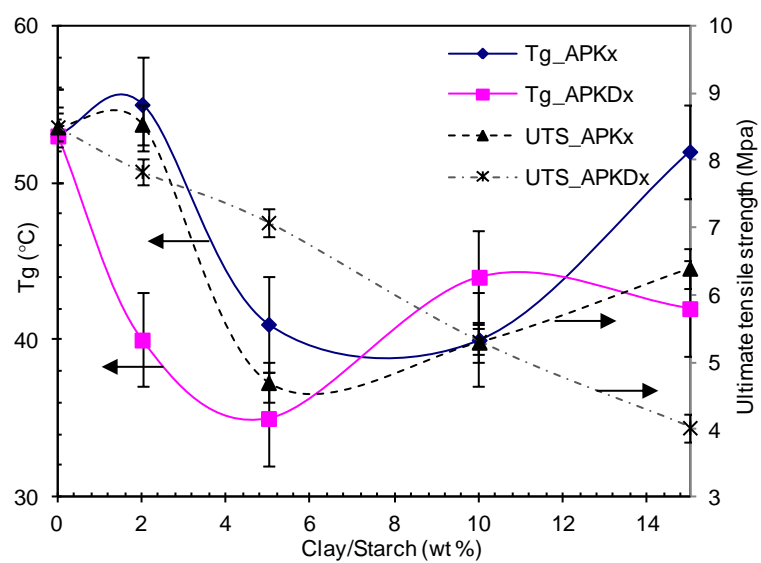


Figure 8: Variation of glass transition temperature (Tg) and ultimate tensile strength (UTS) with clay content.

APKx: films loaded with raw kaolinite and APKDx: films loaded with DMSO intercalated kaolinite